Journal of Sound and Vibration (2001) **248**(1), 71–89
doi:10.1006/jsvi.2001.3775, available online at http://www.idealibrary.com on IDEAL®

A TRANSFER MATRIX APPROACH FOR ACOUSTIC ANALYSIS OF A MULTILAYERED ACTIVE ACOUSTIC COATING

C. Cai, G. R. Liu and K. Y. Lam

Institute of High Performance Computing, 89-*C Science Park Drive* #02-11/12, *The Rutherford*, *Singapore Science Park* 1, *Singapore* 118261, *Singapore. E-mail: caic@ihpc.nus.edu.sg*

(*Received* 14 *April* 2000, *and in final form* 26 *March* 2001)

A transfer matrix approach is presented to evaluate and analyze the acoustic characteristics of a multilayered active acoustic coating, which can be applied to actively reduce sound reflection and/or transmission upon a given sound wave excitation. Expressions are derived to obtain the reflection and transmission coefficients, and to separate the incident sound pressure with reflected sound pressure from two integrated piezoelectric sensor layers. Numerical results for reflection and transmission coefficients of three cases are presented to verify the approach and to depict its effectiveness in the field of study and simulation of a multilayered active acoustic coating with a backing plate.

1. INTRODUCTION

Piezoelectric materials can transform mechanical energy into electric energy and *vice versa*. On the one hand, they strain when an electric field is applied across them; on the other, they produce a voltage (electrically polarized) under stress. The first effect is called the converse piezoelectric effect and the latter is called the direct piezoelectric effect [1]. The converse piezoelectric effect allows one to use the piezoelectric devices as actuators, while the latter makes them well suited as sensors. These properties together with their small size and weight allow one to apply the piezoelectric materials to construct smart devices that can be used for active sound and vibration control. It is a common practice to use piezoelectric ceramics of lead zirconate titanate (PZT) compositions for sensor and actuator applications in smart structures [2]. For example, the cancellation of a reflected acoustic is to set up a destructive interference condition with the sound wave as it is reflected from the termination "wall" [3]. This technique was improved by coating sheets of piezoelectric polymers to act as the sensors in a host encapsulant over the actuator [4]. One multilayered coating structure usually includes both sensors and actuator(s). The sensor devices detect the incident sound wave and output electrical signals in terms of the incident sound wave. The output signal (amplitude and phase) from the sensors is fed into a control circuit that is then used to drive the actuator device to develop a destructive acoustic pressure response for cancellation of the reflected sound wave.

An active acoustic coating with bilaminar actuators was introduced which could cancel both the reflection and transmission of normally incident sound waves simultaneously [5]. The analysis of the coating was presented based on the Mason equivalent circuit representation (MECR). The input signals to the actuators were obtained by the separated hydrophone that was placed in front of the coating. Lafleur and co-workers [6, 7] built the

0022-460X/01/460071 + 19 $35.00/0

equation relating the reflection or transmission coefficients of a layer of piezorubber to the driving voltage applied across the layer based on a one-dimensional model by Auld [1]. The calculated results were also compared to the values from measurements. Photiadis *et al* [8] presented a simple centre-of-mass representation (SCMR) for a double-layer actuator, which can provide a direct view of the actuator operation. Furthermore, the authors extended this technique to study the influence of backing compliance on the performance of surface mounted actuator [9] and to predict the acoustic characteristics of each transducer component [10].

All the methods, such as MECR, one-dimensional model [6, 7] and SCMR, are suitable for one- or two-layer coating. In reality, the active acoustic coating consists of multilayers such as actuator, pressure sensor, velocity sensor, waterproofing, bonding and other layers. To obtain an integrated coating with good and predictable performance, all the layers in the coating, whether they are passive layers, sensor layers or actuator layers, must be analyzed with consideration of all coupling and interaction conditions simultaneously.

The acoustic analysis of a multilayered active coating has not been reported previously. The purpose of this paper is to systematically describe the theory behind the applications of piezoelectric materials for sound reflection and/or transmission control. A technique based on the transfer matrix approach [11, 12] is presented in order to predict the acoustic performance of the multilayered active coating. Two cases are used to demonstrate the effectiveness of the technique. Finally, an eight-layer active coating with backing plate is studied to show the application of the proposed transfer matrix approach.

2. PIEZOELECTRIC MATERIALS

In this section, the piezoelectric material properties are summarized. In particular, attention is focused on a piezoelectric layer with the poling direction normal to the layer (z direction). Both direct and converse piezoelectric effects are assumed to be linear phenomena.

At constant electric field strength, the mechanical characteristics are defined by

$$\boldsymbol{\sigma} = \mathbf{c}^E \boldsymbol{\varepsilon}, \tag{1}$$

where $\boldsymbol{\sigma}$ and $\boldsymbol{\varepsilon}$ are the stress and strain vectors, respectively, and $\mathbf{c}^E$ denotes the elastic matrix. The superscript E indicates that the value is measured with constant electric field.

At constant mechanical strain, the electrical characteristics are defined by

$$\mathbf{D} = \mathbf{g}^S \mathbf{E}, \tag{2}$$

where $\mathbf{E}$ is the electric field vector, $\mathbf{D}$ is the electric displacement vector and $\mathbf{g}^S$ the dielectric matrix [13, 14]. The superscript S indicates that the value is measured at constant mechanical strain.

The piezoelectric characteristics (direct piezoelectric effect), at constant electric field are defined by

$$\mathbf{D} = \mathbf{e}\boldsymbol{\varepsilon} \tag{3}$$

and the piezoelectric characteristics (converse piezoelectric effect) at constant mechanical strain, by

$$\boldsymbol{\sigma} = -\mathbf{e}^{\mathrm{T}} \mathbf{E}, \tag{4}$$

where $\mathbf{e}^{\mathrm{T}}$ is the transpose of $\mathbf{e}$, the piezoelectric stress matrix or the dielectric permittivity matrix.

By combining two piezoelectric effects together with equations (1) and (2), the global constitute relations of piezoelectric material can be written as

$$\boldsymbol{\sigma} = \mathbf{c}^{E}\boldsymbol{\varepsilon} - \mathbf{e}^{\mathrm{T}}\mathbf{E}, \qquad \mathbf{D} = \mathbf{e}\boldsymbol{\varepsilon} + \mathbf{g}^{S}\mathbf{E}. \tag{5, 6}$$

There is, in passing, a relation between the piezoelectric stress matrix $\mathbf{e}$ and the elastic matrix $\mathbf{c}$ via the piezoelectric strain matrix $\mathbf{d}$, which is often provided by the manufacturer of piezoelectric materials, $\mathbf{e} = \mathbf{dc}$.

3. GOVERNING EQUATIONS

It is helpful to begin with the assumption that the active coating is infinitive in extent. The thin layer structure, in which the thickness of the layer is orders of magnitude smaller than its transverse dimensions, can be well approximated by the infinite layer. Consider the coating consisting of an arbitrary number N of passive layers and piezoelectric active laminae perfectly bonded at their interfaces and stacked normal to the z direction of a Cartesian system (x, y, z), x–y plane is chosen to coincide with the bottom surface of the coating. Here, the stacking of the layers is restricted such that the x and y directions coincide with their principle axes. Several assumptions are applied in the following analysis:

(1) Physical properties of the bonding materials in the coating are negligible.
(2) The electrodes with negligible physical properties are perfectly conductive.
(3) The piezoelectric coupling is weak.
(4) The fluid (water and/or air) does not support piezoelectric effects, i.e., its electricity potential is zero. This implies that the electric potential of the coating vanishes at the coating–fluid interface or the electrodes are short-circuited.

A steady monochromatic wave with angular frequency ω and time dependence $\mathrm{e}^{\mathrm{i}\omega t}$ impinges the coating normally. With this choice of co-ordinate system and sound incident direction mentioned above, the displacement would reduce to a one-dimensional vector. The remaining field variables will be independent of x and y.

A voltage V_z is applied onto the two electrodes on the piezoelectric layer polarized along axis z as shown in Figure 1. The electric and mechanical effects on the response of the layer to a sound excitation are considered separately. First, the state variables caused by purely mechanical effects are considered. For a simple one-dimensional problem with z poling direction of piezoelectric materials, the governing equations for a layer are simplified in the case of absence of body force as [15–21]

$$\rho\ddot{w} - c_{33}\frac{\partial^2}{\partial z^2}w = 0, \qquad \sigma_z^m = c_{33}\frac{\partial w}{\partial z}, \tag{7, 8}$$

where w is the displacement of the layer, ρ the density, c_{33} the elastic stiffness constant. Superscript m denotes the mechanical effect.

From equations (7) and (8), the state variables on the upper and lower faces of the layer have the following relations:

$$\sigma_1^m = \mathrm{j}\frac{\rho v}{\tan(kd)}v_1 - \mathrm{j}\frac{\rho v}{\sin(kd)}v_2, \qquad \sigma_2^m = \mathrm{j}\frac{\rho v}{\sin(kd)}v_1 - \mathrm{j}\frac{\rho v}{\tan(kd)}v_2, \tag{9, 10}$$

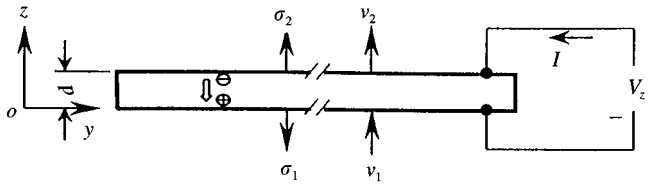

Figure 1. The co-ordinates and state variables at the top and bottom faces of a layer.

where σ_1, v_1 and σ_2, v_2 symbolize the normal stresses and velocities at lower and upper faces of the layer respectively. $k = \sqrt{(\rho/c_{33})}\omega$ is the wavenumber, $v = \sqrt{c_{33}/\rho}$ the velocity of longitudinal elastic (acoustic) waves travelling in the thickness direction of the layer and d the thickness of the layer. $\mathrm{j} = \sqrt{-1}$.

Secondly, the state variables caused by an external voltage V_z (or electric field E) applied across the piezoelectric layer are considered. Sign conventions are chosen in accordance with normal circuit practice as shown in Figure 1. The stress generated by the converse piezoelectric effect is from equation (4).

$$\sigma_z^e = -e_{33}E_z, \tag{11}$$

where superscript e denotes the piezoelectric effect.

As the layer is very thin, the electric field can be treated as constant with the layer thickness direction. The relation between the applied electric field and terminal voltage is

$$V_z = \int_0^d E_z \,\mathrm{d}z = \mathrm{d}E_z. \tag{12}$$

The electrical terminal current is calculated by [1]

$$I = \mathrm{j}\omega D_z A, \tag{13}$$

where A is the area of the piezoelectric layer.

Due to the assumption of weak piezoelectric coupling, the self-generated voltage (direct effect from the excitation of acoustic waves) can be neglected when considering the actuator layers [22]. Therefore, it leads to, from equation (2),

$$E_z = \frac{D_z}{g_{33}}. \tag{14}$$

Substitution of equations (15) and (14) into equation (11) yields

$$\sigma^e = \mathrm{j}\,\frac{e_{33}}{g_{33}\omega A}\,I. \tag{15}$$

The compound stresses by mechanical effect and electric effect together will be

$$\sigma_1 = \sigma_1^m + \sigma^e = \mathrm{j}\,\frac{\rho v}{\tan(kd)}\,v_1 - \mathrm{j}\,\frac{\rho v}{\sin(kd)}\,v_2 + \mathrm{j}\,\frac{e_{33}}{g_{33}\omega}\,J, \tag{16}$$

$$\sigma_2 = \sigma_2^m + \sigma^e = \mathrm{j}\,\frac{\rho v}{\sin(kd)}\,v_1 - \mathrm{j}\,\frac{\rho v}{\tan(kd)}\,v_2 + \mathrm{j}\,\frac{e_{33}}{g_{33}\omega}\,J, \tag{17}$$

where $J = I/A$.

The total voltage on the electrodes including the external applied voltage and self-generated voltage because of direct piezoelectric effect will be from equations (12), (6) and (13):

$$V_z = \int_0^d \frac{1}{g_{33}}(D_z - e_{33}\varepsilon_z)\,\mathrm{d}z = \frac{1}{g_{33}}\int_0^d \left(\frac{I}{\mathrm{j}\omega A} - e_{33}\frac{\partial w}{\partial z}\right)\mathrm{d}E \tag{18}$$

$$= \mathrm{j}\frac{e_{33}}{\omega g_{33}}v_2 - \mathrm{j}\frac{e_{33}}{\omega g_{33}}v_1 - \mathrm{j}\frac{d}{\omega g_{33}}J.$$

Presenting equations (16), (17) and (18) in matrix form leads to

$$\begin{Bmatrix}\sigma_1\\ \sigma_2\\ V_z\end{Bmatrix} = \begin{bmatrix} z_{11} & z_{12} & z_{13}\\ -z_{12} & -z_{11} & z_{13}\\ -z_{13} & z_{13} & z_{33}\end{bmatrix}\begin{Bmatrix}v_1\\ v_2\\ J\end{Bmatrix}, \tag{19}$$

where

$$z_{11} = \mathrm{j}\frac{\rho v}{\tan(kd)}, \qquad z_{12} = -\mathrm{j}\frac{\rho v}{\sin(kd)}, \qquad z_{13} = \mathrm{j}\frac{e_{33}}{g_{33}\omega}, \qquad z_{33} = -\mathrm{j}\frac{d}{g_{33}\omega}. \tag{20}$$

Equation (19) can be used to describe the purely elastic layer, actuator layer and sensor layer.

$J = V_z = 0$	for purely elastic layer,
$J = 0$ and $V_z \neq 0$	for purely sensor layer and V_z is the voltage output from the layer,
$J \neq 0$ and $V_z \neq 0$	for actuator layer, which means that there exists an external voltage input.

4. TRANSFER MATRICES OF THE DIFFERENT LAYERS

For elastic layer n,

$$\begin{Bmatrix}\sigma_2\\ v_2\end{Bmatrix}_n = \begin{bmatrix} 0 & z_{12}\\ -1 & -z_{11}\end{bmatrix}^{-1}\begin{bmatrix}1 & -z_{11}\\ 0 & z_{12}\end{bmatrix}\begin{Bmatrix}\sigma_1\\ v_1\end{Bmatrix}_n = \mathbf{TM}_{0n}\begin{Bmatrix}\sigma_1\\ v_1\end{Bmatrix}_n. \tag{21}$$

Subscripts 2 and 1 attached to the state variables denote the upper and lower surface of the current layer respectively. $\mathbf{TM}_{0n}$ is named the main transfer matrix of the layer n.

For sensor layer n, the main transfer matrix has the same form as the elastic one but the sensor layer has an extra expression for its voltage output as follows:

$$V_{sn} = z_{13}\{-1 \quad 1\}\begin{Bmatrix}v_1\\ v_2\end{Bmatrix}_n = \mathbf{TM}_{sn}\begin{Bmatrix}v_1\\ v_2\end{Bmatrix}_n. \tag{22}$$

For actuator layer a, substituting equation (19) into equations (17) and (18) will result in

$$\begin{Bmatrix}\sigma_2\\ v_2\end{Bmatrix}_a = \begin{bmatrix} 0 & \left(z_{12}-\dfrac{z_{13}^2}{z_{33}}\right)\\ -1 & -\left(z_{11}+\dfrac{z_{13}^2}{z_{33}}\right)\end{bmatrix}^{-1}\begin{bmatrix} 1 & -\left(z_{11}+\dfrac{z_{13}^2}{z_{33}}\right)\\ 0 & \left(z_{12}-\dfrac{z_{13}^2}{z_{33}}\right)\end{bmatrix}\times\left(\begin{Bmatrix}\sigma_1\\ v_1\end{Bmatrix}_a - \frac{z_{13}}{z_{33}}\begin{Bmatrix}1\\ 1\end{Bmatrix}_a V_a\right) \quad (23)$$

$$= \mathbf{TM}_{1a}\begin{Bmatrix}\sigma_1\\ v_1\end{Bmatrix}_a + \mathbf{TM}_{2a}V_a,$$

where V_a is the external voltage applied. $\mathbf{TM}_{1a}$ and $\mathbf{TM}_{2a}$ are named the first and second matrices of actuator layer.

5. WAVE FIELD IN THE FLUIDS

There exist two kinds of plane sound waves in the upper fluid. One is the incident sound wave and the other is the sound wave reflected by the active coating. They can be expressed, respectively, as

$$p^{in} = \bar{p}^{in}\mathrm{e}^{\mathrm{i}k_2 z}, \qquad p^{re} = \bar{p}^{re}\mathrm{e}^{-\mathrm{j}k_2 z} = R\bar{p}^{in}\mathrm{e}^{-\mathrm{j}k_2 z}. \quad (24a, 24b)$$

The particle velocities caused by the sound waves are respectively

$$v^{in} = -\frac{k_2}{\omega\rho_2}p^{in}, \qquad v^{re} = \frac{k_2}{\omega\rho_2}R\bar{p}^{in}\mathrm{e}^{-\mathrm{j}k_2 z}. \quad (25a, 25b)$$

There exists only a down-going plane sound wave in the lower fluid, assuming that the fluid goes to infinity in the negative z direction. The transmitted plane wave can be expressed as

$$p^{tr} = \bar{p}^{tr}\mathrm{e}^{\mathrm{j}k_1 z} = T\bar{p}^{in}\mathrm{e}^{\mathrm{j}k_1 z}, \qquad v^{tr} = -\frac{k_1}{\omega\rho_1}T\bar{p}^{in}\mathrm{e}^{\mathrm{j}k_1 z}, \quad (26a, 26b)$$

where k_1, k_2, ρ_1 and ρ_2 are the wave numbers and densities in the lower and upper fluids respectively, R and T are sound reflection and transmission coefficients respectively.

6. INTERACTION CONDITIONS

To solve the problems, the governing equations must be applied together with additional boundary conditions for the sought-for electrical, mechanical and acoustic quantities. In electroelasticity theory, mechanical boundary conditions are formulated just like in the classical elasticity theory: the stresses, displacements or mixed boundary conditions are specified at the boundary of each layer. When the piezoelectric layer is perfectly bonded on the mechanical structure, the strain equals to the corresponding one of the structure at the interface.

Therefore, continuity of velocities and stresses requires ω to be the same in all layers and in upper and lower fluids. Three coupling and boundary conditions are

(1) On the interface between the upper fluid and the coating laminae

$$\begin{Bmatrix}\sigma_2\\ v_2\end{Bmatrix}_1 = \begin{Bmatrix}-(1+R)\\ \dfrac{R-1}{\rho_2 C_2}\end{Bmatrix}\bar{p}^{in}, \quad n=1. \tag{27}$$

(2) On the interfaces between the layers of the coating laminae

$$\begin{Bmatrix}\sigma_1\\ v_1\end{Bmatrix}_n = \begin{Bmatrix}\sigma_2\\ v_2\end{Bmatrix}_{n+1}, \quad 1 \leqslant n \leqslant (N-1). \tag{28}$$

(3) On the interface between the lower fluid and the coating laminae

$$\begin{Bmatrix}\sigma_1\\ v_1\end{Bmatrix}_N = -\begin{Bmatrix}1\\ \dfrac{1}{\rho_1 C_1}\end{Bmatrix}\bar{p}^{in}T, \quad n=N. \tag{29}$$

7. APPLICATION EXAMPLES

Based on the transfer matrices of elastic, sensor and actuator layers above, as well as continuous interaction conditions, the reflection and transmission coefficients of any multilayered coating can be carried out straightforwardly. The relationship of acoustic characteristics of the active acoustic coating to the voltages applied across the actuator layers can also be analyzed. Three cases are studied below. The first two cases are for the purpose of verification.

Case 1: *Lafleur's example* [6]. The calculated results for the examples given by Lafleur have been compared to the results from experimental ones. Therefore, those examples are used here for the purpose of verification. The material and structural properties for two kinds of smart structures are listed in Table 1. The medium properties above and below the coating laminae are $\rho_1 = \rho_2 = 1000$ kg/m^3 and $C_1 = C_2 = 1500$ m/s respectively. There are two examples for case 1:

(1) Single-layer transducer (Figure 1)
(2) Double-layer transducer (Figure 2)

Figures 3 and 4 show the magnitude and phase of the complex ration of the voltage applied to the single-layered transducer to cancel reflection to that to cancel transmission. Figures 5 and 6 show the magnitude and phase of the complex ration of the voltage on the top layer to that on the bottom layer when the two layers are being driven so as to

TABLE 1

Material and structural properties (*case* 1)

	Piezoelectric material
ρ	5903·3 kg/m^3
c_{33}	$(4{\cdot}92 + j3{\cdot}02) \times 10^9$ N/m^2
e_{33}	$(0{\cdot}2391 + j0{\cdot}0899)$ N/(m V)
g_{33}	$(0{\cdot}3857 - j0{\cdot}0119) \times 10^{-9}$ F/m
Thickness	525×10^{-6} m

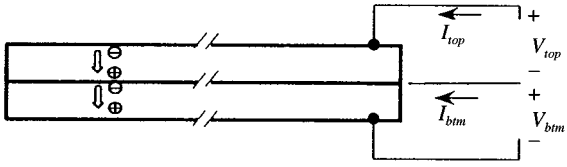

Figure 2. Double-layer transducer with a plane wave incident from the top.

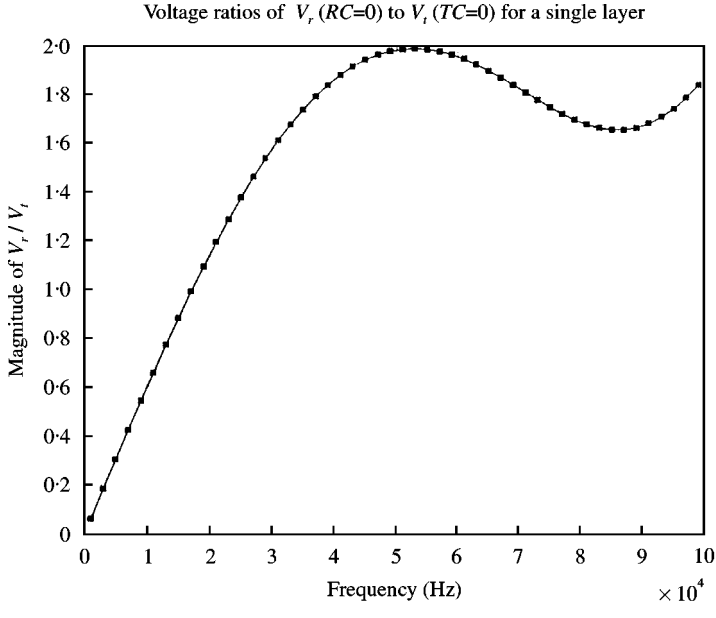

Figure 3. Magnitude of the complex ratio of the voltage for cancelling reflection to one for cancelling transmission with the single active layer: ———, TM results; ■ ■ ■, Lafleur's.

simultaneously cancel both transmission and reflection from the double-layer transducer. It can be found that the results from the proposed transfer matrix method in this paper are in good agreement with the calculated results by Lafleur.

Case 2: *Bao's example* [3]. Bao's example is used because his analysis was carried out based on the method of MECR. The bilaminar actuator is constructed by using two layers of piezoceramic composite material together as shown in Figure 7. The material and structural properties used are listed in Table 2. The medium properties above and below the coating laminae are $\rho_1 = \rho_2 = 1000\ \text{kg/m}^3$ and $C_1 = C_2 = 1500\ \text{m/s}$ respectively.

The calculated ratios of the magnitude and phases for the applied voltages as a function of frequency are plotted in Figures 8 and 9. Good agreement is also observed.

Case 3: *The coating with two sensor layers and an actuator layer.* The calculated results are relative values unless the incident sound wave is assumed to be a known value. In practice, amplitude, phase and frequency of the incident sound wave are not known in advance. Hence, the properties of incident sound wave need to be measured or detected. That is why the sensors or sensoring devices are usually integrated into the active acoustic coating.

In case 3, an active acoustical coating with eight layers is considered as shown in Figure 10. The material properties used are listed in Table 3. Two sensor layers (layers 2 and 4) are

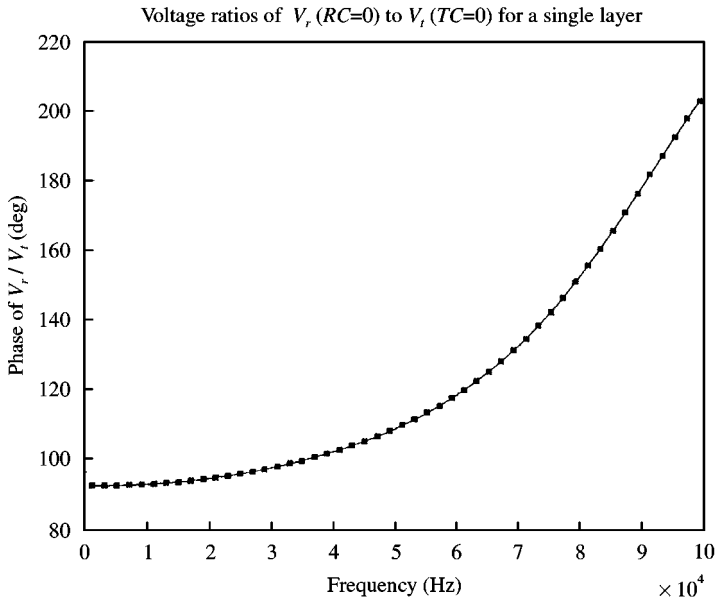

Figure 4. Phase of the complex ratio of the voltage for cancelling reflection to one for cancelling transmission with the single active layer: ———, TM results; ■ ■ ■, Lafleur's.

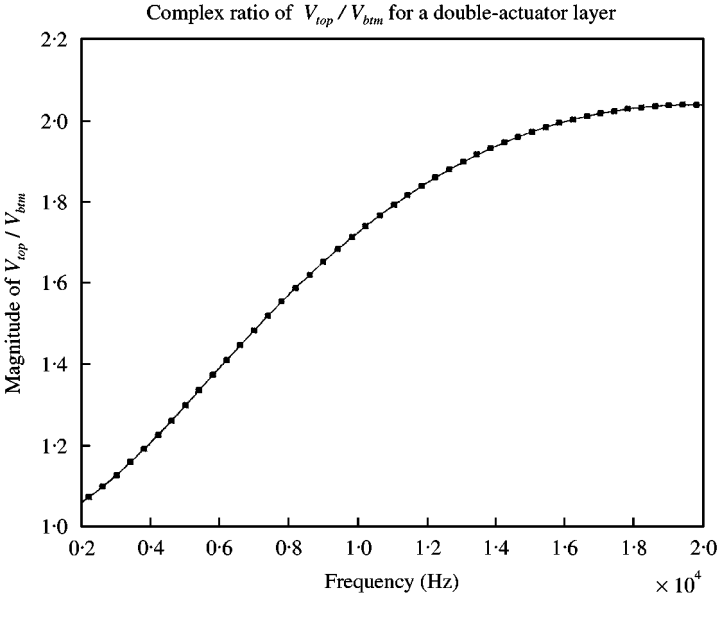

Figure 5. Magnitude of the complex ratio of the voltages on the top layer to that on the bottom layer for cancelling reflection and transmission with the double active layer: ———, TM results; ■ ■ ■, Lafleur's.

made of PVDF material with the same thickness 515×10^{-6} m. The actuator layer (layer 6) is PZT-5 rod in a Rho-C rubber matrix with a thickness of 0·02 m. The thickness of the elastomeric layers is 0·002 m, and the thickness of the backing plate is 0·01 m. The medium properties above are $\rho_2 = 1000$ kg/m^3 and $C_2 = 1500$ m/s. The medium properties below are $\rho_1 = 1{\cdot}18$ kg/m^3 and $C_1 = 340$ m/s.

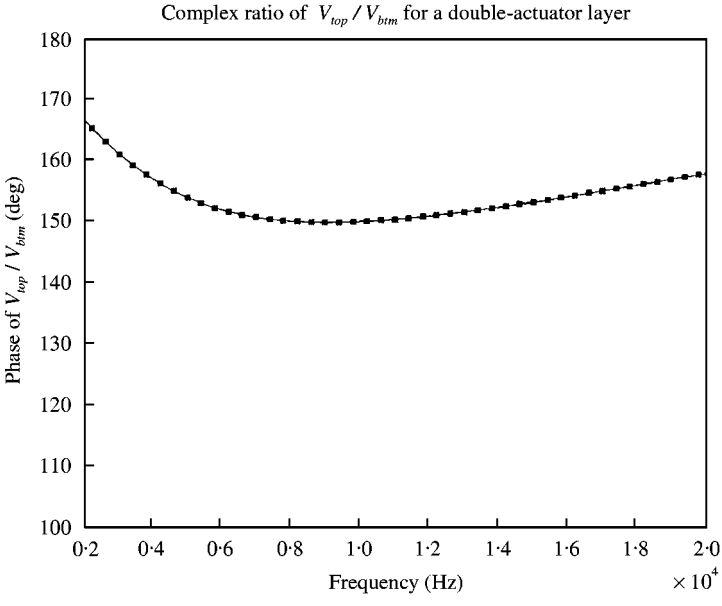

Figure 6. Phase of the complex ratio of the voltages on the top layer to that on the bottom layer for cancelling reflection and transmission with the double active layer: ———, TM results; ■ ■ ■, Lafleur's.

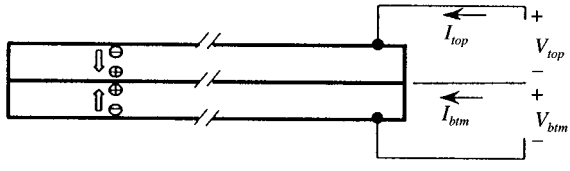

Figure 7. A bilaminar actuator.

TABLE 2

Material and structural properties (*case* 2)

	Piezoelectric material
ρ	2430 kg/m^3
c_{33}	$2{\cdot}3791 \times 10^9$ N/m^2
e_{33}	3·95 N/(m V)
g_{33}	$1{\cdot}543 \times 10^{-9}$ F/m
Thickness	0·02 m

Based on the continuity of velocities and stresses at each interface, respectively, one can obtain

$$\begin{Bmatrix} -(1+R) \\ \dfrac{R-1}{\rho_2 C_2} \end{Bmatrix} \bar{p}^{in} = \mathbf{TM}_{01}\mathbf{TM}_{02}\mathbf{TM}_{03}\mathbf{TM}_{04}\mathbf{TM}_{05} \times \left(-\mathbf{TM}_{16}\mathbf{TM}_{07}\mathbf{TM}_{08} \begin{Bmatrix} 1 \\ \dfrac{1}{\rho_1 C_1} \end{Bmatrix} \bar{p}^{in} T + \mathbf{TM}_{26} V_{a6} \right). \tag{30}$$

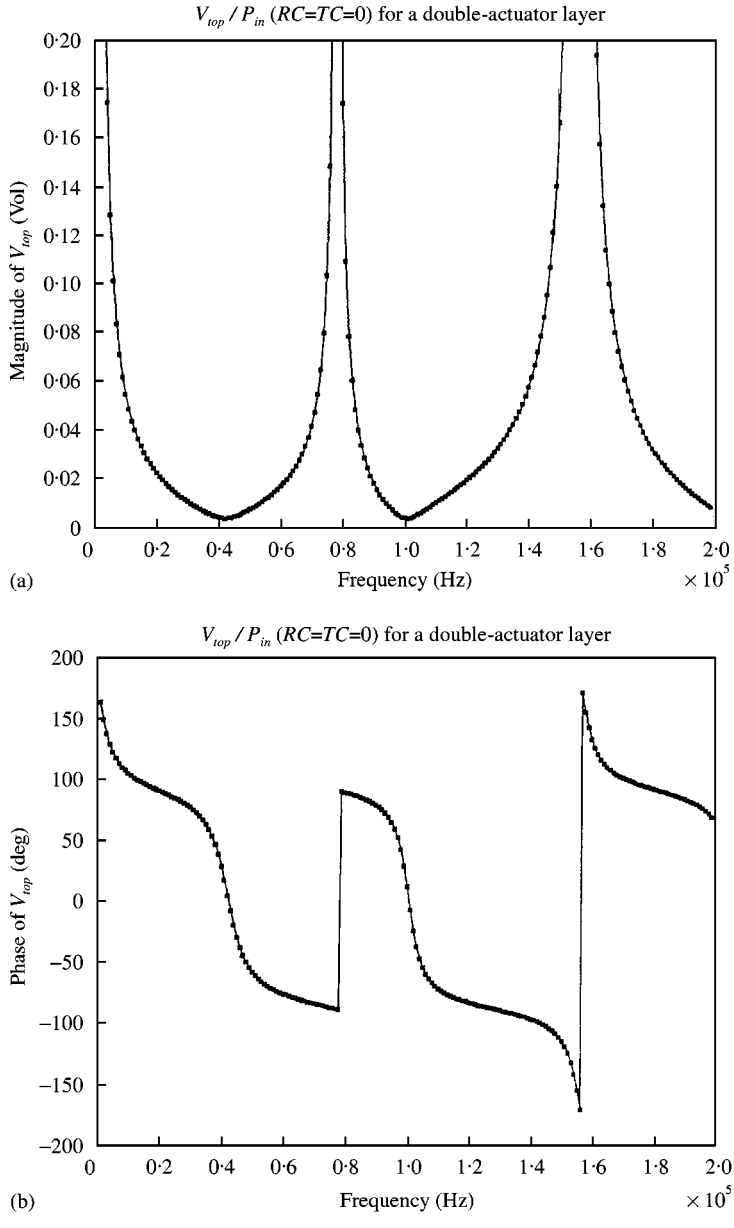

Figure 8. The applied voltage on the upper layer required for the condition $TC = RC = 0$: (a) the magnitude of the applied voltage on the upper layer and (b) the phase of the applied voltage on the upper layer: ———, TM results; ■ ■ ■, Bao's.

From equation (22), voltage outputs from the two sensors are, respectively,

$$V_{s2} = \mathbf{TM}_{s2} \begin{Bmatrix} v_1 \\ v_2 \end{Bmatrix}_2 \quad \text{and} \quad V_{s4} = \mathbf{TM}_{s4} \begin{Bmatrix} v_1 \\ v_2 \end{Bmatrix}_4. \tag{31}$$

The reason double sensor layers are used here is that the output of a sensor is a signal in terms of the complete acoustic field that includes both incident and reflected sound. It

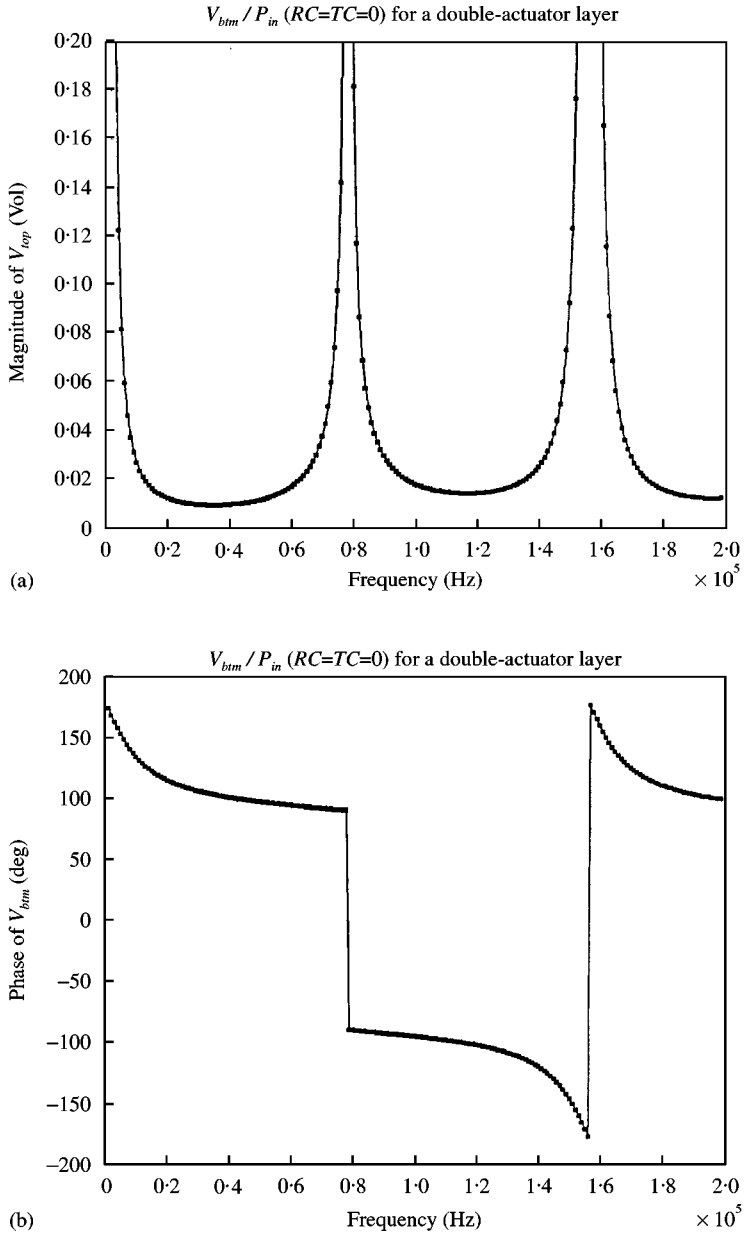

Figure 9. The applied voltage on the lower layer required for the condition $TC = RC = 0$: (a) the magnitude of the applied voltage on the lower layer and (b) the phase of the applied voltage on the lower layer. ———, TM results; ■ ■ ■, Bao's.

means that components of the incident and reflected sound pressures are summed together in the output of a single sensor layer. The resulting signal is therefore a superposition of the two components. Therefore, the dual arrangement is preferred for separating the incident sound wave [23, 24]. The dual sensor may be in other forms, such as one sensor layer for sound pressure and one accelerometer for particle velocity [10].

The incident (p^{in}) and reflected (p^{re}) sound waves can be obtained in terms of the voltages V_{s2} and V_{s4} generated through the direct piezoelectric effect of the two sensors. The pressures

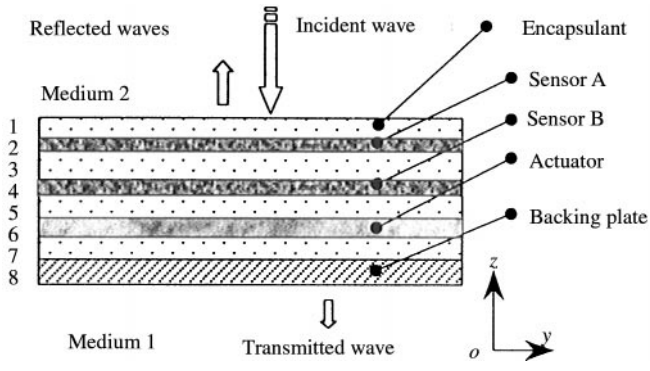

Figure 10. A backing plate covered by a coating with integrated sensors and an actuator.

TABLE 3

Material and structural properties (*case* 3)

	Elastomer layer [ρC rubber (isotropic)]	
ρ	920 kg/m^3	
c_{33}	$2{\cdot}4132 \times 10^9$ N/m^2	
Thickness	0·002 m	
	Sensor layer [PVDF (transversely isotropic)]	Actuator layer
ρ	1470 kg/m^3	2430 kg/m^3
c_{33}	$1{\cdot}5306 \times 10^9$ N/m^2	$2{\cdot}3791 \times 10^9$ N/m^2
e_{33}	3·7 N/(m V)	3·95 N/(m V)
g_{33}	$6{\cdot}729 \times 10^{-11}$ F/m	$1{\cdot}543 \times 10^{-9}$ F/m
Thickness	515×10^{-6} m	0·02 m
	Backing plate (isotropic)	
ρ	7800 kg/m^3	
c_{33}	$268{\cdot}47 \times 10^9$ N/m^2	
Thickness	0·01 m	

at sensors 2 and 4 are represented as a superposition of the incident and reflected field.

$$V_{s2} = S_p(p^{in}\mathrm{e}^{-\mathrm{j}k_1d_1} + p^{re}\mathrm{e}^{\mathrm{j}k_1d_1}), \tag{32}$$

$$V_{s4} = S_p(p^{in}\mathrm{e}^{-\mathrm{j}k_1d_1}\mathrm{e}^{-\mathrm{j}(k_2d_2+k_3d_3)} + p^{re}\mathrm{e}^{\mathrm{j}k_1d_1}\mathrm{e}^{\mathrm{j}(k_2d_2+k_3d_3)}), \tag{33}$$

where the exponential factors above account for the phase difference, k_i and d_i are the wavenumber and thickness of layer $i(i = 1, 2$ or 3) respectively. S_p represents the acoustic pressure sensitivity or voltage–pressure transfer function of the matched sensors, which can be expressed as

$$S_p = \frac{\text{Open-circuit output voltage of the sensor}}{\text{Free-field plane wave sound pressure}} \tag{34}$$

in units of V/Pa.

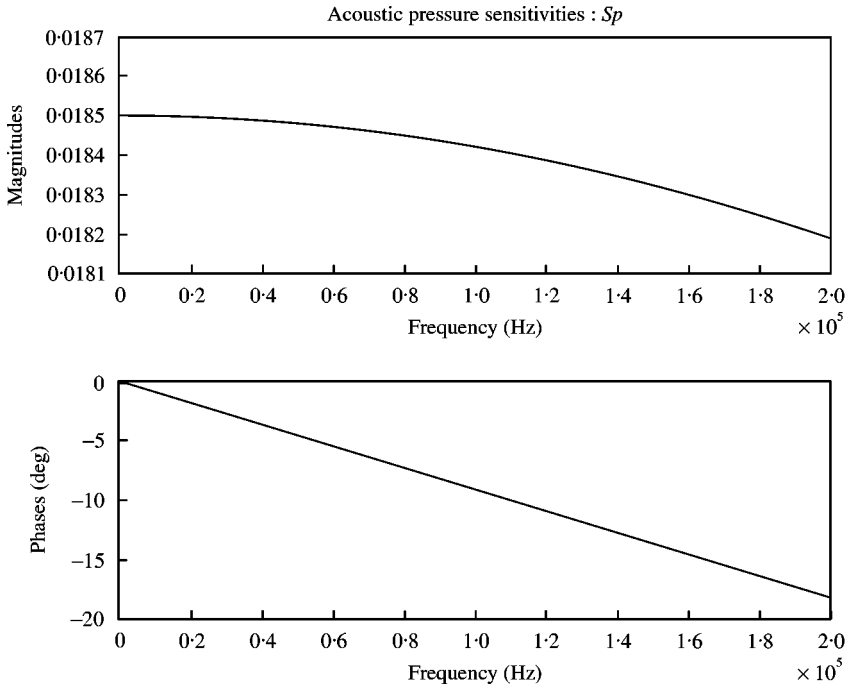

Figure 11. Acoustic pressure sensitivity of a single sensor layer.

For the given piezoelectric material as shown in Table 3, the acoustic pressure sensitivity of a single sensor is shown in Figure 11. To obtain the incident sound pressure, some manipulation is needed as follows:

$$V_{si} = V_{s4}\mathrm{e}^{-\mathrm{j}(k_2d_2+k_3d_3)} - V_{s2} \tag{35}$$

$$= S_p p^{in}\mathrm{e}^{-\mathrm{j}k_1d_1}(\mathrm{e}^{-2\mathrm{j}(k_2d_2+k_3d_3)} - 1);$$

therefore,

$$p^{in} = \mathrm{j}\,\frac{V_{si}}{2S_p\sin(k_2d_2 + k_3d_3)\mathrm{e}^{-\mathrm{j}(k_2d_2+k_3d_3)}}\,\mathrm{e}^{\mathrm{j}k_1d_1}. \tag{36}$$

As an instance, the incident sound pressure calculated from the voltage outputs of the two sensors shown in Figure 10 is verified assuming a known incident pressure. The results are plotted in Figure 12. It is seen that the calculated incident sound pressure has a good accuracy. The accuracy of the above derivation depends on the material selection of sensor layer and elastomer layer [25]. The derivation of equations (32) and (33) is based on an implied assumption that the materials of the first four layers are acoustically transparent. It means that the specific acoustic impedances of these materials should be the same as the medium fluid. For this case study, the specific acoustic impedance of the medium is $1{\cdot}50 \times 10^6$ Pa s/m, while that of the elastomer layer is $1{\cdot}49 \times 10^6$ Pa s/m. The result disagreement in Figure 12 may be attributed to the difference of the specific acoustic impedances. The effect of material on the accuracy of calculation will be discussed in another paper.

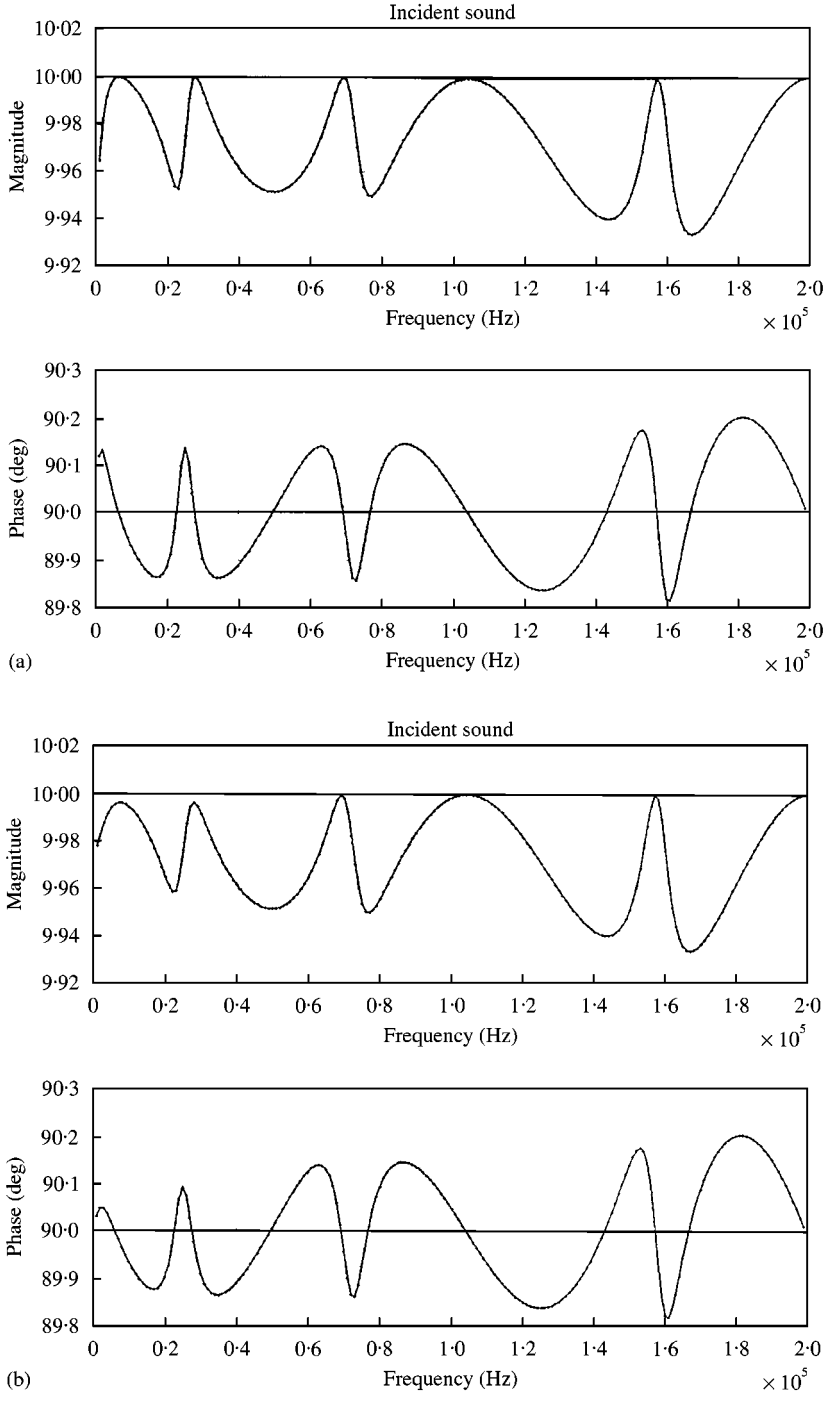

Figure 12. The comparison of calculated and actual incident sound wave: (a) upper medium is water and lower is air and (b) upper medium is water and lower is water. ———, given p^{in}; - - - - - -, calculated p^{in} from two sensors.

Similarly, by shifting the detected signal received at sensor 2 in another way, the reflected sound wave can be obtained as

$$V_{sr} = V_{s4}\mathrm{e}^{\mathrm{j}(k_2d_2+k_3d_3)} - V_{s2} \tag{37}$$

$$= S_p p^{re}\mathrm{e}^{\mathrm{j}k_1d_1}(\mathrm{e}^{\mathrm{j}2(k_2d_2+k_3d_3)} - 1),$$

$$p^{re} = -\,\mathrm{j}\,\frac{V_{sr}}{2S_p\sin(k_2d_2 + k_3d_3)\mathrm{e}^{\mathrm{j}(k_2d_2+k_3d_3)}}\,\mathrm{e}^{-\mathrm{j}k_1d_1}. \tag{38}$$

From equation (30), the transmission and reflection coefficients for a calculated p^{in} will be

$$T = \frac{2 + (TV_1 + TV_2(\rho_2C_2))V_{a6}/p^{in}}{TM(1,1) + TM(1,2)/(\rho_1C_1) + (\rho_2C_2)TM(2,1) + (\rho_2C_2)/(\rho_1C_1)TM(2,2)}, \tag{39}$$

$$R = -1 - TV_1\,\frac{V_{a6}}{p^{in}} + \left(TM(1,1) + \frac{TM(1,2)}{(\rho_1C_1)}\right)T, \tag{40}$$

where

$$\begin{bmatrix} TM(1,1) & TM(1,2) \\ TM(2,1) & TM(2,2) \end{bmatrix} = -\,\mathbf{TM}_{01}\mathbf{TM}_{02}\mathbf{TM}_{03}\mathbf{TM}_{04}\mathbf{TM}_{05}\mathbf{TM}_{16}\mathbf{TM}_{07}\mathbf{TM}_{08},$$

$$\begin{Bmatrix} TV_1 \\ TV_2 \end{Bmatrix} = \mathbf{TM}_{01}\mathbf{TM}_{02}\mathbf{TM}_{03}\mathbf{TM}_{04}\mathbf{TM}_{05}\mathbf{TM}_{26}.$$

To cancel the sound reflection, $R = 0$, we have the required voltage to be applied across the actuator layer from equations (39) and (40) as

$$V_{a6}^{R=0} = \frac{AA}{BB}\,p^{in}, \tag{41}$$

where

$$AA = TM(1,1) + TM(1,2)/(\rho_1C_1) - (\rho_2C_2)TM(2,1) - (\rho_2C_2)/(\rho_1C_1)TM(2,2),$$

$$BB = (TM(1,1) + TM(1,2)/(\rho_1C_1) + (\rho_2C_2)TM(2,1) + (\rho_2C_2)/(\rho_1C_1)TM(2,2))TV_1$$

$$-\,(TV_1 + (\rho_2C_2)TV_2)(TM(1,1) + TM(1,2)/\rho_1C_1).$$

To cancel the sound transmission, $T = 0$, we have the required voltage to be applied across the actuator layer from equations (39) and (40) as

$$V_{a6}^{T=0} = -\,\frac{2}{TV_1 + TV_2(\rho_2C_2)}\,p^{in}. \tag{42}$$

Two control-voltage functions of an active coating are defined as

$$CVF_{R=0} = \frac{AA}{BB}, \tag{43}$$

$$CVF_{T=0} = -\,\frac{2}{TV_1 + TV_2(\rho_2C_2)}, \tag{44}$$

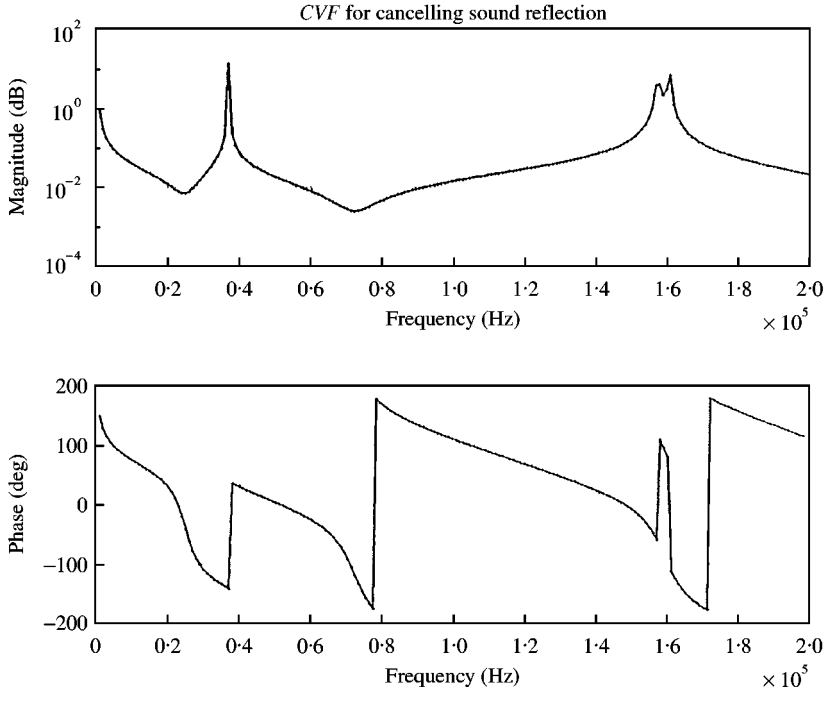

Figure 13. Control-voltage function for cancelling sound reflection.

where $CVF_{R=0}$ and $CVF_{T=0}$ are the control-voltage functions of the active coating for cancelling sound reflection and sound transmission respectively.

Equations (43) and (44) give the relation between the incident sound and control-voltage required applied across the actuator. They depend only on the material and geometrical properties of the coating structure and the media. The control-voltage function for the cancellation of sound reflection is shown for the given eight-layer coating in Figure 13. It is observed from the figure that the given active coating is suitable to cancel the sound reflection in the frequency range 50–130 kHz because poles exist at frequencies 38 and 158 kHz. From the control-voltage functions, the required control voltages can be easily calculated through multiplication, in respective frequencies, of control-voltage function and incident sound that may be obtained by the integrated sensors.

The mechanism for the cancellation of reflected sound waves lies in that the surface that faces the incident sound wave is controlled to move 180° out of phase with and at the same amplitude as the particle velocity of reflecting wave. Another way of viewing this is that the acoustic impedance of the active surface is controlled to dynamically match one of the propagating mediums of the incident side. It means that the incident sound wave travels into the boundary as if it is an infinite medium with the same properties.

8. CONCLUSIONS

The transmission and reflection coefficients from a multilayered active acoustic coating that covers a backing plate submerged in the fluids are investigated using a transfer matrix

approach. In the formulation, the coupling between the fluids, coating with a backing plate and piezoelectric effects is taken into account. The formulation for detecting the incident sound pressure using dual piezoelectric sensor layers is also presented. With the formulation presented, the control-voltage functions of the active coating with a backing plate can be written out directly. The algorithm makes the control circuit easy to be implemented. The product of incident sound that can be detected and the control-voltage functions of active coating with the backing plate is the controlled voltage required for the active control purpose.

As verification, two case studies (Lafleur and Bao's examples) are carried out and it is found that the proposed transfer matrix approach has a good accuracy. The main advantage that lies in the proposed method is that it can be easily applied for analyzing the acoustic properties of multilayer active coating structures. Finally, an eight-layer active structure is analyzed. Its control-voltage functions either for cancelling the sound reflection or for the sound transmission are obtained.

REFERENCES

1. B. A. AULD 1990 *Acoustic Fields and Waves in Solids*, Florida: Krieger Publishing Co., second edition Vol. 1, 326–333.
2. R. Y. TING, T. R. HOWARTH and R. L. GENTILMAN 1996 *Proceedings of SPIE—The International Society for Optical Engineering* (*Smart Structures and Materials* 1996—*Industrial and Commercial Applications of Smart Structures Technologies* 27–29 *February*, 1996 *San Diego*, *CA*), Vol. 2721, 214–221. Underwater evaluation of piezocomposite panels as active surfaces.
3. X.-Q. BAO, V. K. VARADAN and V. V. VARADAN 1988 *Journal of the Acoustical Society of America* **84** (Suppl. 1), S49. Active acoustic absorber for plane waves in water.
4. T. R. HOWARTH, X. Q. BAO, V. K. VARADAN and V. V. VARADAN 1989 *Journal of the Acoustical Society of America* **85** (Suppl. 1), S92. Large area sensors for active acoustic control systems.
5. X.-Q. BAO, V. K. VARADAN, V. V. VARADAN and T. E. HOWARTH 1990 *Journal of the Acoustical Society of America* **87**, 1350–1352. Model of a bilaminar actuator for active acoustic control systems.
6. L. D. LAFLEUR, F. D. SHIELDS and J. E. HENDRIX 1991 *Journal of the Acoustical Society of America* **90**, 1230–1237. Acoustically active surfaces using piezorubber.
7. F. D. SHIELDS and L. D. LAFLEUR 1997 *Journal of the Acoustical Society of America* **102**, 1559–1566. Smart acoustically active surfaces.
8. D. M. PHOTIADIS, J. A. BUCARO and R. D. CORSARO 1994 *Journal of the Acoustical Society of America* **96**, 1613–1619. Double layer actuator.
9. R. D. CORSARO and R. M. YOUNG 1995 *Journal of the Acoustical Society of America* **97**, 2849–2854. Influence of backing compliance on transducer performance.
10. R. D. CORSARO, B. HOUSTON and J. A. BUCARO 1997 *Journal of the Acoustical Society of America* **102**, 1573–1581. Sensor-actuator tile for underwater surface impedance control studies.
11. G. R. LIU, J. TANI, K. WATANABE and T. OHYOSHI 1990 *Journal of Applied Mechanics* **57**, 923–929. Lamb wave propagation in anisotropic laminates.
12. G. R. LIU, K. Y. LAM and H. M. SHANG 1995 *Composite Engineering*: *An International Journal* **5**, 1489–1498. A new method for analysing wave fields in laminated composite plate: two-dimensional cases.
13. M. V. GANDHI and B. S. THOMPSON 1993. *Smart Materials and Structures*. New York: Chapman & Hall.
14. G. CELENTANO and R. SETOLA 1999 *Journal of Sound and Vibration* **223**, 483–492. The modelling of a flexible beam with piezoelectric plates for active vibration control.
15. C. CAI, G. R. LIU and K. Y. LAM 2000 *Applied Acoustics* **61**, 95–109. An exact method for analysing sound reflection and transmission by anisotropic laminates submerged in fluids.
16. G. R. LIU, C. CAI and K. Y. LAM 2000 *Journal of Sound and Vibration* **230**, 809–824. Sound reflection and transmission of compliant plate-like structures by a plane sound wave excitation.
17. G. R. LIU and J. TANI 1994 *Transactions of the American Society of Mechanical Engineers* **116**, 440–448. Surface waves in functionally gradient piezoelectric plates.

18. G. R. LIU and J. TANI 1992 *Transactions of the Japan Society of Mechanical Engineers* **58A**, 504–507. SH surface waves in functionally gradient piezoelectric material plates (in Japanese).
19. X. Q. PENG, K. Y. LAM and G. R. LIU 1998 *Journal of Sound and Vibration* **209**, 635–650. Active vibration control of composite beams with piezoelectrics: a finite element model with third-order theory.
20. G. R. LIU, X. Q. PENG, K. Y. LAM and J. TANI 1997 *Proceedings of the International Conference on Material and Mechanics* '97, 20–22 July 1997, Japan. Modelling of laminated composite plates with integrated piezoelectric sensors and actuators, 539–544.
21. G. R. LIU, Y. L. ZHOU, K. Y. LAM, X. Q. PENG and J. TANI 1997 *Proceedings of the Eighth International Conference on Adaptive Structures and Technologies, Japan*, 29–31 October 1997, 113–122. Finite element modelling of piezoelectric sensors and actuators bonded in thick composite laminates.
22. H. S. TZOU 1992 *Intelligent Structural Systems*. (H. S. Tzou and G. L. Anderson, editors), 9–74. Dordrecht: Kluwer Academic Publishers. Active piezoelectric shell continua.
23. T. R. HOWARTH, V. K. VARADAN, X. Q. BAO and V. V. VARADAN 1992 *Journal of the Acoustical Society of America* **91**, 823–831. Piezocomposite coating for active underwater sound reduction.
24. T. R. HOWARTH, V. K. VARADAN and V. V. VARADAN 1992 *Intelligent Structural Systems* (H. S. Tzou and G. L. Anderson, editors), 285–304. Dordrecht: Kluwer Academic Publishers. Intelligent sensor systems for underwater acoustic applications.
25. M. B. MOFFETT, J. M. POWERS and J. C. MCGRATH 1986 *Journal of the Acoustical Society of America* **80**, 375–381. A ρc hydrophone.